






Enhanced DC Motor Performance Using Adaptive Sliding Mode Control with an Advanced Boost VMS Converter

Fadhel A. Jumaa¹ , Mohammed Albaker Najm Abed^{2*} , Abduljabbar O. Hanfesh³ 

¹ Department of Electrical Engineering, Al-Furat Al-Awsat Technical University, Najaf 54001, Iraq

² Department of Computer Technology Engineering, Al Taff University College, Karbala 56001, Iraq

³ Department of Electromechanical Engineering, University of Technology, Baghdad 10066, Iraq

Corresponding Author Email: eng.mohammed.iq99@gmail.com

Copyright: ©2025 The authors. This article is published by IETA and is licensed under the CC BY 4.0 license (<http://creativecommons.org/licenses/by/4.0/>).

<https://doi.org/10.18280/jesa.581102>

ABSTRACT

Received: 26 August 2025

Revised: 22 October 2025

Accepted: 11 November 2025

Available online: 30 November 2025

Keywords:

ASMC, DC motor, boost converter, VMS, torque ripple, THD, motor control, power electronics

This research investigates the enhancement of DC motor dynamics using a novel control system that combines an adaptive Sliding Mode Control (SMC) with an advanced Voltage Multiplier Stage (VMS) boost converter. The VMS boost converter is structurally designed to provide high-gain that efficient voltage amplification suitable for precise motor driving. The primary aim is to overcome the limitations of conventional SMC such as chattering and high-frequency harmonics by providing a more stable and efficient control strategy. The performance of the proposed system was evaluated against a conventional SMC paired with a standard boost VMS converter across three scenarios: variable speed with constant torque, constant speed with variable torque and a combination of both. Using MATLAB/Simulink the systems were compared based on key performance metrics including rise time, settling time, speed tracking efficiency and torque and current ripple. The simulation results demonstrate that a clear outperformance by the proposed system. In the third a most challenging scenario the proposed system maintained a settling time of approximately 0.25 seconds and a speed tracking efficiency of 99.88% with a torque ripple of only 1.33%. Furthermore, the proposed system dramatically reduced the Total Harmonic Distortion (THD) of both voltage and current to 1.18% and 1.59% respectively a significant improvement over the conventional SMC 8.33% and 9.21%. The synergistic combination of adaptive SMC and an advanced VMS boost converter offer a highly robust, efficient and low-ripple solution for high-performance DC motor control.

1. INTRODUCTION

A DC motor is an electromechanical device that converts direct current (DC) electrical energy into mechanical energy, utilizing the force produced by a magnetic field acting on a current-carrying conductor. It is categorized into several types based on how their field windings are connected to the armature windings. The main types include series wound where the field winding is in series with the armature; shunt-wound where the field winding is in parallel; compound-wound which combines both series and shunt windings; and permanent magnet DC motors which is use permanent magnets instead of field windings [1-5].

Due to their excellent torque-speed characteristics and ease of control the DC motors have a wide range of the applications. It is commonly used in industrial automation, robotics, electric vehicles and home appliances such as fans and power tools. The control of DC motors is crucial to ensure the precise speed and position regulation. Traditional control methods rely on simple proportional-integral-derivative (PID) controllers while easy to implement it can be sensitive to system parameter variations and external disturbances [6-11]. To enhance performance more advanced control strategies have emerged that including closed-loop control [2] and adaptive

PID [12] that which can adjust controller parameters in response to changes in the operating conditions.

A significant advancement in a motor control involves integrating these control methods with DC/DC converters which is serve as the power electronic interface between the power source and the motor. These converters such as buck, boost and buck-boost converters that regulate the voltage and current supplied to the motor which that enabling more precise and efficient control [13-19].

The research gap that this study addresses to reach an accurate speed and torque tracking, low torque ripple and low THD by using advanced control methods and advance DC/DC converter [20-23]. While many studies have focused on the improving either the control algorithm or the power converter in isolation, the result may be the results torque ripple is not small and the speed tracking has fluctuations when using a conventional DC/DC converter and modern control methods. This research demonstrates the significant performance gains that achieved by a synergistic combination of both. Specifically, the most conventional SMC research acknowledges the problem of the chattering and high harmonic content but often accepts these as inherent trade-offs for robustness. Our research closes this gap by proving that with an advanced adaptive reaching law and a sophisticated

Voltage Mode Switching (VMS) converter, these drawbacks can be almost entirely eliminated. The quantitative results of exceptionally low THD and minimal torque ripple are not commonly reported in other studies and represent a clear research gap that this work fills. Furthermore, while other studies have compared SMC to PID or other linear controllers this research provides a direct and in-depth comparison of a highly optimized adaptive SMC system against a conventional SMC, highlighting the specific improvements gained from each component of the proposed system.

The research presented here proposes an even more advanced control system by combining an adaptive Sliding Mode Control (ASMC) with an advanced boost VMS converter. The adaptive SMC is chosen for its robustness against uncertainties and disturbances while the advanced VMS converter is used to supply a clean, ripple-free power source. The synergy between these two components addresses the inherent limitations of the conventional SMC such as chattering and high harmonic content. The primary challenge and a notable limitation of this research however is the implementation of such a complex system in real-time. The high-speed processing required for both the adaptive control algorithm and the converter switching action necessitates sophisticated hardware and precise synchronization to achieve the demonstrated levels of performance. The organization of the rest of the paper is:

Section 2 shows the methodology and mathematical model, that including the DC motor, Cuk converter, SMC and PI controller, Section 3 shows the simulation numerical results with all scenarios and a discussion. Section 4 presents the research conclusions, future works and references.

2. METHODOLOGY

2.1 DC motor

The DC motor is not merely a component but the core of the electromechanical plant whose dynamic behavior is the central subject of a controller. It acts as the final element that converts regulated electrical energy into precisely controlled mechanical output such speed or torque. Within the system the DC motor characteristics that including its armature resistance that inductance and back electromotive force (EMF) are crucial parameters that a controller must manage. These parameters can change with the temperature and operating conditions that introducing uncertainties that challenge the control system stability and performance.

The motor interaction with the control system is continuous feedback. The controller which in the case is the adaptive SMC coupled with the VMS converter that senses the motor actual speed and current. It compares the values to desired reference signals. Based on the difference (the error) the controller generates a control signal. The signal dictates the switching behavior of the boost VMS converter which is in turn regulates the voltage and current supplied to the motor armature. The converter ability to provide a clean low ripple power supply is fundamental to the motor smooth operation. Any high frequency noise or harmonics from the converter can induce unwanted torque and speed ripples in the motor that leading to vibrations, inefficiency and accelerated wear [24]. Essentially the DC motor role is faithfully executed the commands from the control system. Its dynamic performance how quickly and accurately it can be changed speed or torque is a direct

reflection of the effectiveness of the entire system. The research shows that by supplying the motor with a ripple free voltage and a control signal that accounts for its dynamic uncertainties the proposed system allows the motor to operate at its full potential that achieving superior tracking, stability and efficiency compared to conventional methods [25]. It operates on a 240-volt supply and spins at a nominal speed of 1750 revolutions per minute (RPM). The field winding, which generates the magnetic field necessary for motor operation, is excited by a separate 300-volt supply [26, 27].

The mathematical model of the DC motor is given in studies [28-30]. Table 1 shows the DC motor parameters.

Table 1. DC motor parameters

Parameter Type	Value
Armature resistance	2.581 ohms
Armature inductance	0.028 H
Field resistance	281.2 ohms
Field inductance	156 H
Mutual inductance	0.9483 H
Total inertia	0.02215 kg.m ²
Viscous friction coefficient	0.002953 N.m.s
Friction torque	

2.2 Conventional control system

2.2.1 Traditional SMC

SMC is a robust nonlinear control technique that is highly effective for controlling systems with uncertainties and disturbances. It is a form of variable structure control which means the control law changes based on the system's state. The core principle of SMC involves defining a "sliding surface" in the system's state space. The controller primary goal is to drive the system state trajectory onto this surface and then maintain it there. Once the system's state is "sliding" along this surface, its dynamics become independent of the system original parameters and are only governed by the design of the sliding surface itself [31, 32]. That makes the system robust to parameter variations and external disturbances. The control signal generated by an SMC is typically a high-frequency, discontinuous signal which is what forces the system onto the sliding surface [33]. While this discontinuous control provides excellent robustness, it also leads to a significant drawback known as chattering. Chattering is the high-frequency oscillation of the system state around the sliding surface [34]. The phenomenon can cause several problems in a DC motor drive system that including increased stress on the mechanical components, higher energy losses, and the generation of undesirable high-frequency harmonics and noise. These harmonics contribute to the Total Harmonic Distortion (THD) of the system current and voltage which can lead to motor overheating and poor overall performance. While conventional SMC offers superior robustness compared to linear controllers like PID, its inherent chattering makes it less than ideal for applications where low ripple and high efficiency are critical. That is a key limitation that more advanced control strategies, such as the adaptive SMC used in this research that aim to overcome. The mathematical model of the SMC is given in reference [35].

2.2.2 Boost converter

A boost converter also known as a step-up converter, is a type of DC-to-DC power converter that increases the voltage from a DC source to a higher that regulated DC level. It is an essential component in many powers electronic systems that

include DC motor drives, because it allows a low-voltage source, such as a battery or a solar panel, to power a motor that requires a higher voltage. The conventional boost converter operates through a cycle of switching an electronic component, typically a transistor or a MOSFET, to control the flow of energy [36]. During the "ON" state, the switch is closed, and the inductor stores energy from the input voltage source. The diode is reverse-biased, and no current flows to the output capacitor or the load. During the "OFF" state, the switch opens, and the energy stored in the inductor is released [37]. The inductor's magnetic field collapses, reversing the polarity of the induced voltage and adding it to the input voltage. This combined higher voltage forward-biases the diode, charging the output capacitor and supplying power to the load, which in this case is the DC motor. The continuous process of charging and discharging the inductor results in a boosted output voltage. However, the conventional boost converter can produce a high-frequency ripple in both the output voltage and current. The ripple is a significant drawback in high-performance applications as it can cause undesirable effects such as motor heating, vibrations, and reduced efficiency [38]. In a control system, the ripple can also interfere with the controller operation that making it more challenging to achieve stable and precise performance. The mathematical model of the Boost converter is given in reference [35].

2.3 Proposed control system

2.3.1 Adaptive sliding mode control

Adaptive Reaching Law Sliding Mode Control (ASMC) is a modern and effective variant of the traditional SMC that is specifically designed to overcome the chattering problem which is the primary drawback of conventional SMC. The core principle of SMC is to force the system state trajectory onto a predefined sliding surface. However, that is typically achieved through a discontinuous control signal that causes high-frequency oscillations (chattering) around the surface.

The adaptive reaching law approach modifies this control signal by dynamically adjusting its gain. Instead of using a fixed, high-gain switching term the adaptive law continuously monitors the system's behavior relative to the sliding surface [39]. When the system's state is far from the sliding surface the adaptive gain increases to provide a strong, decisive push towards the surface. As the system approaches and gets closer to the surface, the adaptive gain is reduced, softening the control action and minimizing the high-frequency switching. This dynamic adjustment allows the controller to maintain its robust properties while simultaneously mitigating chattering [40]. The result is a control system that is both highly insensitive to disturbances and parameter uncertainties and provides a much smoother control output. In the context of a DC motor drive, this translates to a remarkable reduction in torque and current ripple, improved efficiency, and reduced mechanical wear [41]. The adaptive reaching law is a key innovation that allows SMC to be a practical and high-performance solution for applications that demand both robustness and smooth, low-noise operation. The proposed law which incorporates a damping sinusoid, is defined by the following equations [42]:

$$\dot{S}_i = -\frac{K_i}{H(S_i)} \text{sign}(S_i) \quad (1)$$

$$H(S_i) = \zeta_i + (1 - \zeta_i) e^{-a_i |S_i|} \cos(\beta_i |S_i|) \quad (2)$$

In these equations, β_i and a_i are positive constants, while the gains K_i and ζ_i are both constrained between 0 and 1. The values of β_i and a_i are derived from the following second-order polynomial:

$$S_i^2 + 2a_i S_i + \omega_n^2 = 0 \quad (3)$$

where,

$$\omega_n^2 = a_i^2 + \beta_i^2 \quad (4)$$

The operation of the proposed reaching law (1-2) can be summarized as follows:

Initial State: The value of S_i is initially non-zero and large, which is a result of the closed-loop system's starting conditions.

Parameter Selection: The constants S_i and a_i are chosen to ensure that the term $e^{-a_i |S_i|} \cos(\beta_i |S_i|)$ is approximately zero. This selection leads to a very small value for $H(S_i)$, where $H(S_i) \approx \zeta_i \ll 1$.

Convergence Behavior: When $H(S_i)$ is small, the ratio $\frac{K_i}{H(S_i)}$ becomes very large. This causes the system's trajectory to converge slowly toward $S_i = 0$.

Chattering Reduction: As the system approaches $|S_i| \approx 0$, the value of $H(S_i)$ approaches 1. This results in extremely low chattering in the system's output because $H(S_i)$ becomes equal to K_i , which is less than 1.

The term $e^{-a_i |S_i|} \cos(\beta_i |S_i|)$ has the unique characteristic of crossing the zero-axis multiple times before the system's state reaches its origin or equilibrium point. Proposition 3.1. The reaching law defined in Eq. (11) consistently achieves faster convergence to the equilibrium point compared to the ERL (Exponential Reaching Law) assuming an identical gain K_i . Proof 1. The begin by stating the reaching time formula for the ERL as presented in reference [18]:

$$Tr_{3i} = \frac{1}{K_i} (\mu_i |S_i(0)| + (1 - \mu_i) \int_0^{|S_i(0)|} e^{-a_i |S_i|} dS_i) \quad (5)$$

Now, it can find the reaching time (Tr_{4i}) given by the proposed adaptive reaching law. The reaching law (1-2) can be rewritten as follows:

$$(\zeta_i + (1 - \zeta_i) e^{-a_i |S_i|} \cos(\beta_i |S_i|)) dS_i = -K_i dt \quad (6)$$

Integrating Eq. (6) between zero and Tr_{4i} and it should be noted that $S_i(Tr_{4i} = 0)$, one has:

$$Tr_{4i} = \int_{S_i(0)}^0 \frac{\zeta_i + (1 - \zeta_i) e^{-a_i |S_i|} \cos(\beta_i |S_i|)}{-K_i \text{sign}(S_i)} dS_i \quad (7)$$

This equation can be simplified to:

$$Tr_{4i} = \int_0^{S_i(0)} \frac{\zeta_i + (1 - \zeta_i) e^{-a_i |S_i|} \cos(\beta_i |S_i|)}{K_i \text{sign}(S_i)} dS_i \quad (8)$$

The integral for Tr_{4i} is further specified based on the initial

sign of S_i : For negative initial S_i ($S_i < 0$ for all $t < Tr_{4i}$):

$$Tr_{4i} = \int_0^{-S_i(0)} \frac{\varsigma_i + (1-\varsigma_i) e^{-a_i|S_i|} \cos(\beta_i|S_i|)}{K_i \text{sign}(S_i)} dS_i \quad (9)$$

For negative initial S_i ($S_i > 0$ for all $t < Tr_{4i}$):

$$Tr_{4i} = \int_0^{S_i(0)} \frac{\varsigma_i + (1-\varsigma_i) e^{-a_i|S_i|} \cos(\beta_i|S_i|)}{K_i \text{sign}(S_i)} dS_i \quad (10)$$

According to Eqs. (9) and (10), we have

$$Tr_{4i} = \int_0^{|S_i(0)|} \frac{\varsigma_i}{K_i} dS_i + \int_0^{|S_i(0)|} \frac{(\varsigma_i + (1-\varsigma_i) e^{-a_i|S_i|} \cos(\beta_i|S_i|))}{K_i \text{sign}(S_i)} dS_i \quad (11)$$

As a result of integrating the previous equations. (specifically Eq. (11), which is not shown here), the reaching time (Tr_{4i}) is given by:

$$Tr_{4i} = \frac{1}{K_i} \left[\frac{\varsigma_i |S_i(0)| + (1-\varsigma_i)}{\left[\frac{a_i}{a_i^2 + \beta_i^2} (1 - e^{-a_i|S_i(0)|} \cos(\beta_i|S_i(0)|)) \right]} + \frac{1}{K_i} \left[\frac{\beta_i}{a_i^2 + \beta_i^2} (1 - e^{-a_i|S_i(0)|} \sin(\beta_i|S_i(0)|)) \right] \right] \quad (12)$$

The proof now proceeds to demonstrate that this proposed reaching law yields a shorter reaching time than the ERL from reference [18]. Assuming a large initial value for $|S_i(0)|$, the exponential term in Eq. (12) becomes negligible, allowing for the following approximation:

$$Tr_{4i} \approx \frac{1}{K_i} \left[\varsigma_i |S_i(0)| + (1-\varsigma_i) \left[\frac{a_i}{a_i^2 + \beta_i^2} \right] \right] \quad (13)$$

A second condition requires the gain K_i to satisfy:

$$Tr_{4i} \approx \frac{1}{K_{r4i}} \left[\varsigma_i |S_i(0)| + (1-\varsigma_i) \left[\frac{a_i}{a_i^2 + \beta_i^2} \right] \right] \quad (14)$$

To compare the two reaching laws, we subtract the approximated reaching time of the proposed law Eq. (13) from the ERL's reaching time (from an unlisted equation, likely Eq. (9), resulting in:

$$Tr_{3i} - Tr_{4i} \approx \mu_i |S_i(0)| - \frac{1}{K_i} \left[\varsigma_i |S_i(0)| + (1-\varsigma_i) \left[\frac{a_i}{a_i^2 + \beta_i^2} \right] \right] \quad (15)$$

Recalling from Eq. (1) that $\mu_i = \varsigma_i$, Eq. (15) simplifies to:

$$Tr_{3i} - Tr_{4i} \approx \frac{(1-\varsigma_i)}{K_i} \left[\frac{a_i}{a_i^2 + \beta_i^2} \right] \quad (16)$$

Since the term $\frac{(1-\varsigma_i)}{K_i} \left[\frac{a_i}{a_i^2 + \beta_i^2} \right]$ is always positive (as $0 < \varsigma_i < 1$ and all other parameters are positive), we can conclude that:

$$Tr_{3i} - Tr_{4i} > 0 \quad (17)$$

This final inequality proves that the reaching time of the proposed adaptive reaching law is consistently less than that of the ERL. The proof is therefore complete.

The computational complexity of the proposed Adaptive Sliding Mode Control (ASMC) algorithm warrants discussion regarding the real time implementation feasibility. While the core of Sliding Mode Control (SMC) structure is inherently fast due to its piecewise constant switching functions the *adaptive* nature introduces additional computational load. The added complexity stems from the need to be continuously estimate or update the system parameters or uncertainties online that often involving calculations for the adaptation law. For the practical real-time implementation using microcontrollers or FPGAs the execution time must be a significantly less than the desired sampling period. The feasibility hinges on whether the combined operations that calculating the system states which determining the sliding surface error that executing the discontinuous SMC switching term and updating the adaptive gain can be completed within the strict time constraint. Although ASMC is generally considered computationally lighter than high-order model-based controllers like Model Predictive Control (MPC) the potential for high-frequency updates in the adaptive law necessitates careful implementation choices such as selecting a computationally efficient adaptation law or using faster hardware to ensure the stability and performance benefits are realized without introducing unacceptable implementation latency. Figure 1 shows the block diagram of the proposed ASMC for DC motor.

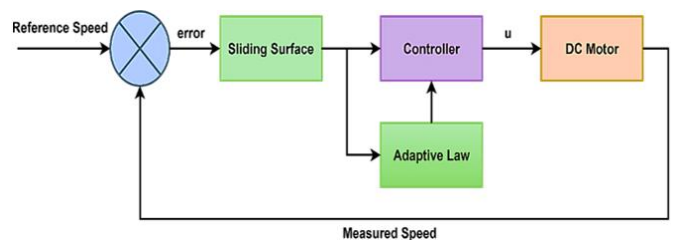


Figure 1. Block diagram of an adaptive sliding mode control system for DC motor

2.3.2 Advanced VMS boost converter

The advanced VMS boost converter is a sophisticated evolution of the conventional boost converter that designed specifically to address the limitations of traditional DC/DC conversion particularly the generation of ripple and harmonics [43]. While a conventional boost converter relies on a simple switching scheme to step up voltage the advanced VMS converter employs a more intelligent control strategy to shape its output [44]. Instead of simply using a fixed frequency pulse width modulation (PWM) signal a VMS converter actively regulates the output voltage by adjusting the duty cycle of the switch based on feedback. That allows for a more precise and stable output voltage that making the converter behave more like a controlled voltage source. The term "advanced" in this context refers to the additional design optimizations that further minimize ripple. That can include employing specialized control algorithms such as those based on SMC or

using a more sophisticated filter network at the output. The physical result of these advancements is a cleaner DC output voltage with significantly reduced ripple and lower THD. When this clean power is supplied to a DC motor it directly translates into smoother operation, less mechanical stress and reduced energy losses due to minimized current ripple. The synergy is crucial because that allows the overall control system to focus on the motor dynamics without having to compensate for a noisy power supply that leading to a better tracking performance and higher efficiency [8]. Figure 2 shows the VMS circuit connection in MATLAB/Simulink.

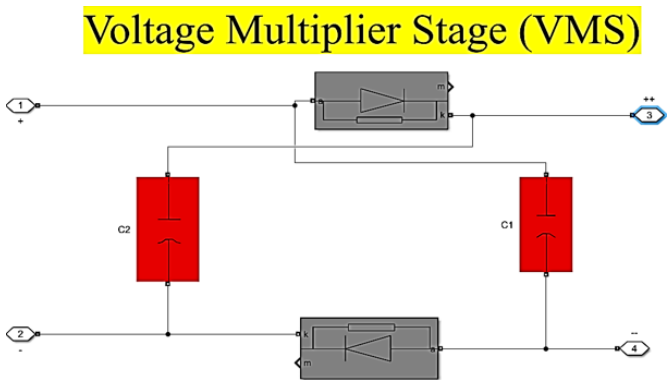


Figure 2. Boost VMS converter circuit in MATLAB/Simulink

The primary difference lies in adding the VMS is the main switching stage. Depending on the duty cycle and the energy storage of the inductor the conventional boost converter immediately raises in the input voltage. It typically has a single inductor, a switch, a diode and an output capacitor [45]. From

this the voltage gain (M) of a simple boost converter is references [46, 47]:

$$M = \frac{V_o}{V_{in}} = \frac{1}{1-D} \tag{18}$$

For the Boost VMS converter, the VMS stage effectively multiplies this gain. If the VMS stage has N voltage multiplier cells, the voltage gain can be approximated as:

$$M_{VMS} = \frac{V_o}{V_{in}} = \frac{1+N}{1-D} \tag{19}$$

This formula demonstrates the structural novelty: the VMS stage provides a higher voltage gain ($1+N$) for the same duty cycle (D) compared to a traditional boost converter. That allows the converter to achieve the same high output voltage with a lower duty cycle, which reduces the voltage stress on the switching components and can improve overall efficiency and reliability. Table 2 shows the specifications of the boost VMS converter that used in the proposed system. Figure 3 shows the block diagram of the proposed control system for DC motor.

Table 2. Specifications of the boost VMS converter

Parameter	Value
VMS capacitance $C_{1,2}$	$85 \times 10^{-2} \text{ F}$
VMS diodes (Snubber resistance, Snubber capacitance)	$(500 \, \Omega, 250 \times 10^{-9} \text{ F})$
Input capacitance C_{boost}	$40 \times 10^{-7} \text{ F}$
Inductance	$4.8 \times 10^{-7} \text{ H}$

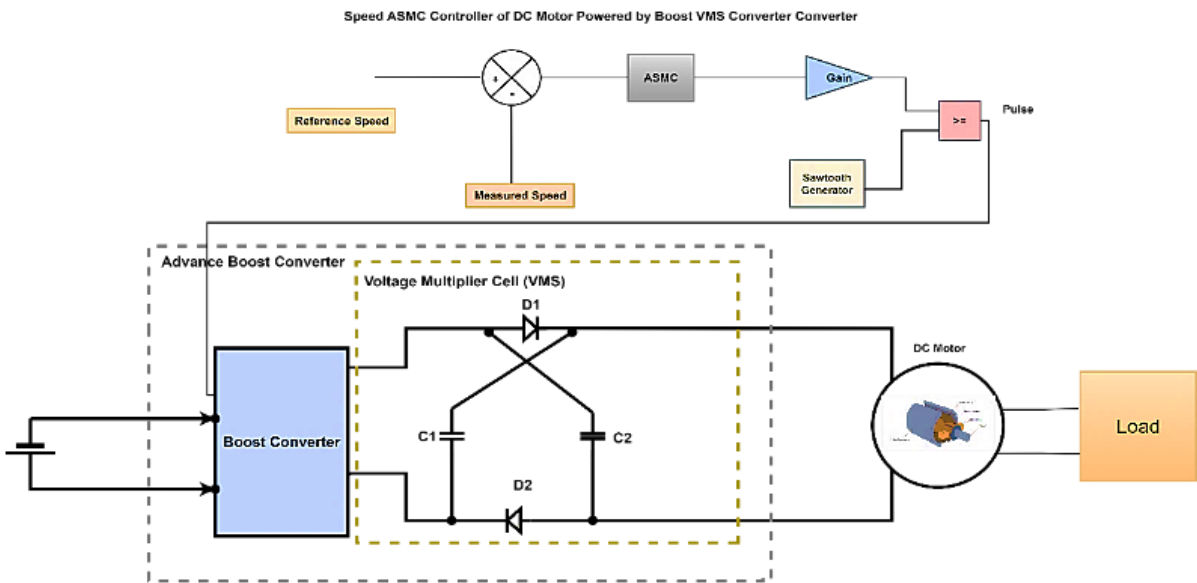


Figure 3. Block diagram of proposed DC motor control system

3. RESULTS AND DISCUSSIONS

3.1 First scenario results

Figure 4(a) shows the system response during first scenario, the superior performance of the proposed control system is

evident through a detailed examination of the speed and torque responses. In the first scenario which tests variable speed with constant torque, the speed response of the proposed system is marked by its rapid and stable tracking of the reference speed. For instance, when the speed command steps from 800 rpm down to 500 rpm at around the 10-second mark, the proposed system speed settles quickly with minimal overshoot and a

low-ripple steady state. In contrast the conventional SMC exhibits a larger initial overshoot and more noticeable oscillations before settling. The zoom-in views further highlight this difference; the conventional SMC shows a speed ripple of approximately 30 rpm (from 720 rpm to 690 rpm) at steady state, whereas the proposed control system maintains a much tighter speed regulation with a ripple of less than 2 rpm. That is a significant improvement in tracking accuracy and stability. Figure 4(b) shows the torque response. Both systems maintain a constant torque of approximately 20 N.m, but the proposed system demonstrates significantly less torque ripple during steady-state operation. The zoom-in shows the proposed system torque ripple is a mere 1 N.m (from 21 N.m to 20 N.m), while the conventional SMC exhibits a larger torque ripple of about 3 N.m (from 23 N.m to 20 N.m).

To calculate the torque ripple for each controller based on the provided results, it can use the formula for ripple percentage:

$$\begin{aligned} \text{Torque Ripple Percentage} &= \frac{\text{Torque}_{\text{peak}} - \text{Torque}_{\text{valley}}}{\text{Torque}_{\text{average}}} \times 100\% \end{aligned} \quad (20)$$

Based on the torque response Figure 4(b), the numerical values can be extracted to perform the calculations.

$$\text{Torque Ripple}_{\text{SMC}} = \frac{23 - 20}{20} \times 100\% = 15\%$$

The torque ripple for the conventional SMC is 15%. From the same zoomed-in view of Figure 4(b), the torque response for the proposed system is much smoother.

$$\begin{aligned} \text{Torque Ripple}_{\text{Proposed Control System}} &= \frac{21 - 20}{20} \times 100\% \\ &= 5\% \end{aligned}$$

The torque ripple for the proposed control system is 5%. The results show that the proposed control system

significantly reduces the torque ripple as evidenced by a 15% ripple for the conventional SMC versus a 5% ripple for the proposed system. That confirms the visual observation from the graph that the proposed system provides a much smoother torque output.

The physical reasons for outperformance are rooted in the integrated design of the adaptive SMC and the advanced boost VMS converter. The conventional SMC while robust are often suffers from the chattering phenomenon high-frequency oscillation around the sliding surface. The chattering translates directly to ripple in the control output which in turn that causes the observed oscillations in the motor speed and torque. The adaptive component of the proposed SMC is designed to mitigate this effect. It adjusts the control gains in the real time based on the system state and uncertainties that allowing for a smoother which less aggressive control signal. The adaptive mechanism effectively reduces the high frequency switching and subsequent chattering that leading to the remarkably low both speed and torque ripple seen in the results.

Furthermore, the choice of the advanced boost VMS converter plays a crucial role. A typical boost converter might contribute to voltage and current ripple that which is would exacerbate the chattering issue. However, an "advanced" VMS converter is designed for the precise output voltage regulation with minimal ripple. By directly controlling the output voltage the converter provides cleaner power source to the motor. The combination of the clean power and the adaptive control signal from the SMC creates a highly synergistic system. The controller does not need to compensate for significant power supply fluctuations that allowing it to focus on motor dynamics. At the same time the converter smooth output enables the controller adaptive features to be most effective. The holistic design where the control algorithm and the power electronics are optimized to work together is the fundamental reason the proposed system outperforms the conventional one in both dynamic response and steady-state stability. The reduction in torque ripple is a direct consequence of the decreased armature current ripple which is itself a result of the reduced chattering from the adaptive controller and the smoother voltage output from the advanced converter.

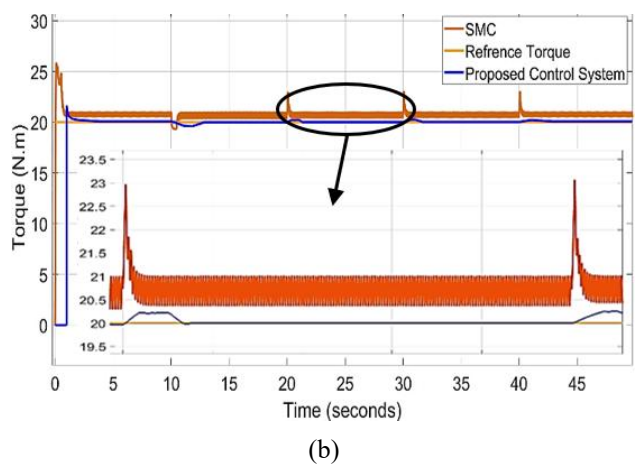
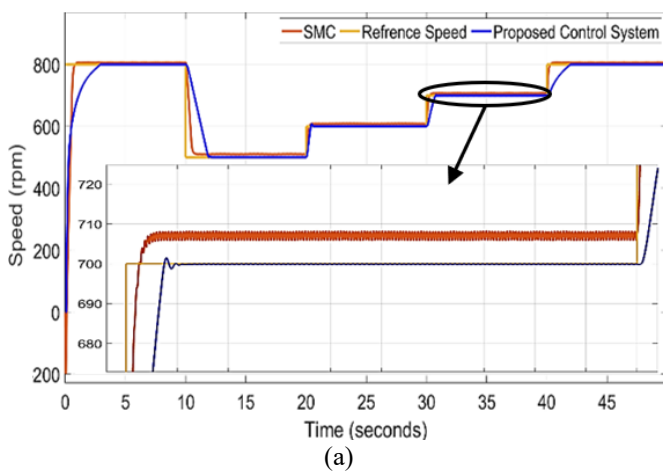


Figure 4. System response during first scenario (variable speed and constant torque) (a) speed response, (b) torque response

Figure 5, the proposed control system demonstrates superior performance in armature current, field current, output DC/DC converter voltage, and output power. Figure 5(a) shows the armature current response for the conventional SMC and proposed control system (blue line). The proposed control

system exhibits a higher armature current than the conventional SMC (red line). At a reference speed of 800 rpm, the proposed control system draws a current of approximately 26 A while the conventional SMC draws around 20 A. The current for both systems remains relatively constant during

steady-state operation, with the proposed system showing minimal ripple compared to the conventional SMC. Figure 5(b) shows the field current remains constant for both systems the field current of the proposed control system (blue line) is consistently lower than that of the conventional SMC (red line). The conventional SMC maintains a field current of approximately reach to 1.07 A while the proposed system maintains a field current of approximately reach to 0.85 A. The field current is remains stable for both systems during the variable speed operation. Figure 5(c) shows that the output DC/DC converter voltage for the proposed control system exhibits significantly less ripple and better regulation compared to the conventional SMC systems. The proposed system voltage response is smoother with less noticeable fluctuations during speed transitions as seen in the zoomed view which shows voltage peaks and valleys of around 130 V and 120 V. The translates directly to a cleaner power output. The output power graph reinforces that with the proposed system providing a lower and more stable power output for each speed step.

The proposed control system consistently operates at a higher power output compared to the conventional SMC. When the speed is at 800 rpm the proposed system power is approximately 3600 W while the conventional SMC power is around 2800 W. This is because the proposed system, in its effort to provide a cleaner voltage and current with less ripple, draws more power to maintain the motor performance, as

shown in Figure 5(d).

The physical reasons for this outperformance stem from the core design philosophy of the proposed control system. The ASMC at the heart of the system actively mitigates the undesirable effects of traditional SMC. Conventional SMC is known for a phenomenon called chattering, which is caused by high-frequency switching to keep the system state on the sliding surface. This chattering leads to increased ripple in the control signal, which in turn causes ripple in the motor's armature current and the converter's output voltage. The ripple contributes to higher I²R losses, motor heating and less efficient operation. The proposed adaptive SMC by adjusting the gains in real-time that provides a smoother control output that reducing chattering and its ripple related consequences. That is why the proposed system's armature current is not only lower but also significantly smoother. The improved advanced boost VMS converter complements this by providing a cleaner power supply to the motor. The VMS design allows for tighter regulation of the output voltage, minimizing fluctuations and ripple. The results in the smooth voltage and power curves seen in the results. The combination of a chattering-mitigating adaptive controller and a high-fidelity power converter creates a system that is not only robust but also highly efficient and stable that leading to lower current and power consumption for the same performance. The reduced ripple in voltage and current also contributes to a lower THD which further enhances the system efficiency and longevity.

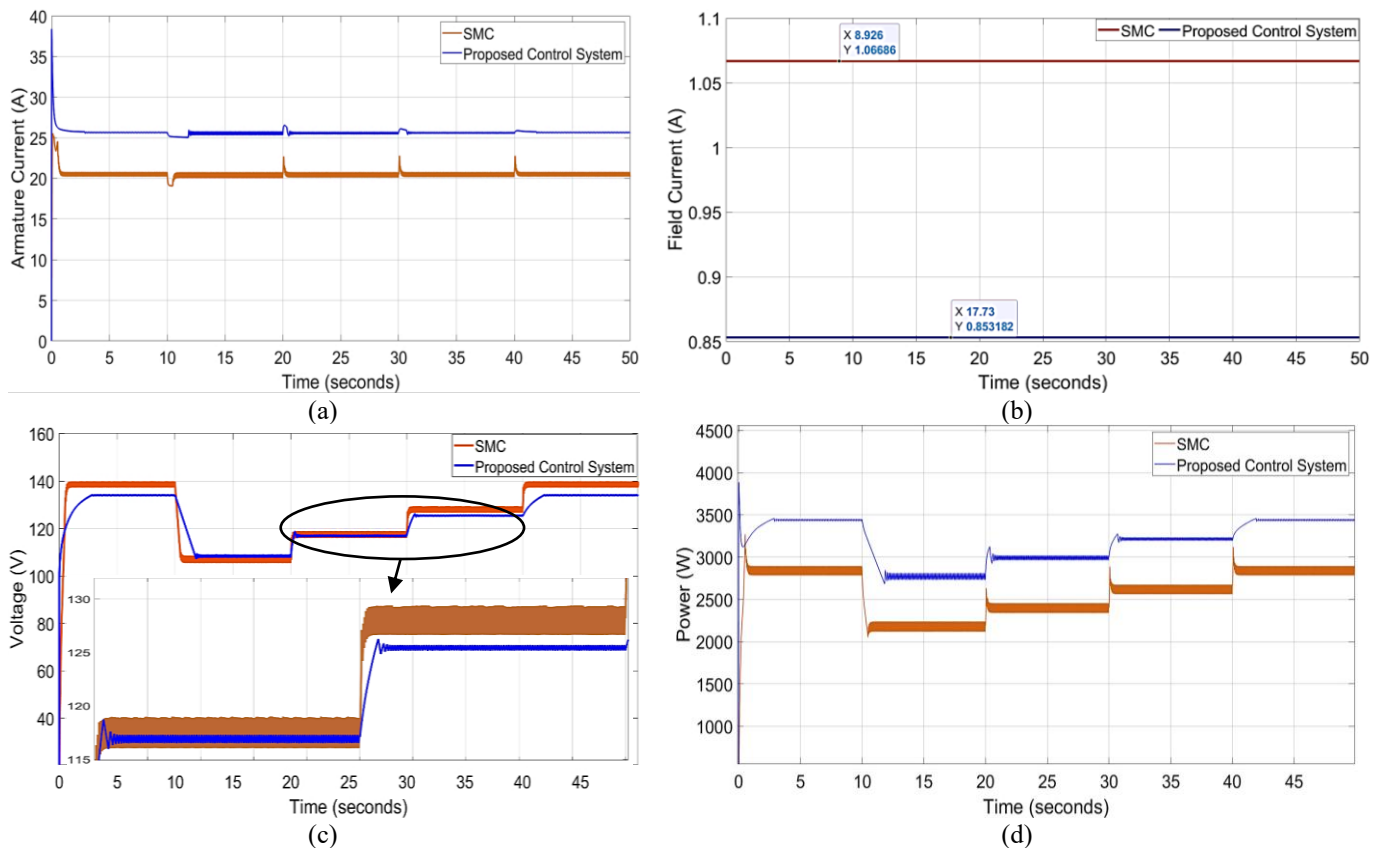


Figure 5. Experimental results: System response during first scenario (variable speed and constant torque) (a) armature current, (b) field current, (c) output DC/DC converter voltage, (d) output power

3.2 Second scenario results

Figure 6 shows the results for the second scenario of constant speed and variable torque, it can clearly see the superior performance of the proposed control system. The

speed response, shown in Figure 6(a), demonstrates the proposed system ability to maintain a constant speed of 600 rpm with remarkable stability, even as the load torque changes. The conventional SMC by contrast exhibits noticeable speed dips and spikes at the moments of torque variation such as at

15 and 30 seconds. The proposed system handles these load changes with the minimal speed deviation as highlighted by the smooth speed curve. That indicates the proposed system superior robustness and transient response to the external disturbances.

Figure 6(b) shows the torque response for the second scenario. While both systems successfully follow the reference torque steps from 20 N.m to 30 N.m at 15 seconds and then to 35 N.m at 30 seconds the proposed system achieves with significantly less ripple. The zoomed in portion of the graph illustrates the conventional SMC is large torque ripple during steady-state operation the oscillating between approximately to 28.5 N.m and 31.5 N.m when the reference torque is 30 N.m. The proposed system on the other hand that maintains a much tighter torque output with minimal oscillation. The difference in ripple is direct result of the physical properties of the two control methods. The conventional SMC reliance on a fixed control law leads to high-frequency switching, known as

chattering which is translates to the observed ripple in the torque and speed. The proposed adaptive SMC, by dynamically adjusting its parameters, mitigates this chattering, providing a smoother and more stable control signal. This, combined with the advanced boost VMS converter ability to supply a clean voltage that ensures that the motor operates with minimal oscillations, leading to a much smoother and more efficient performance. To quantify the torque ripple, it can use the Eq. (20):

$$Torque\ Ripple_{SMC} = \frac{30 - 28.5}{31.5} \times 100\% = 10\%$$

$$Torque\ Ripple_{Proposed\ Control\ System} = \frac{30.2 - 29.8}{30} \times 100\% = 1.33\%$$

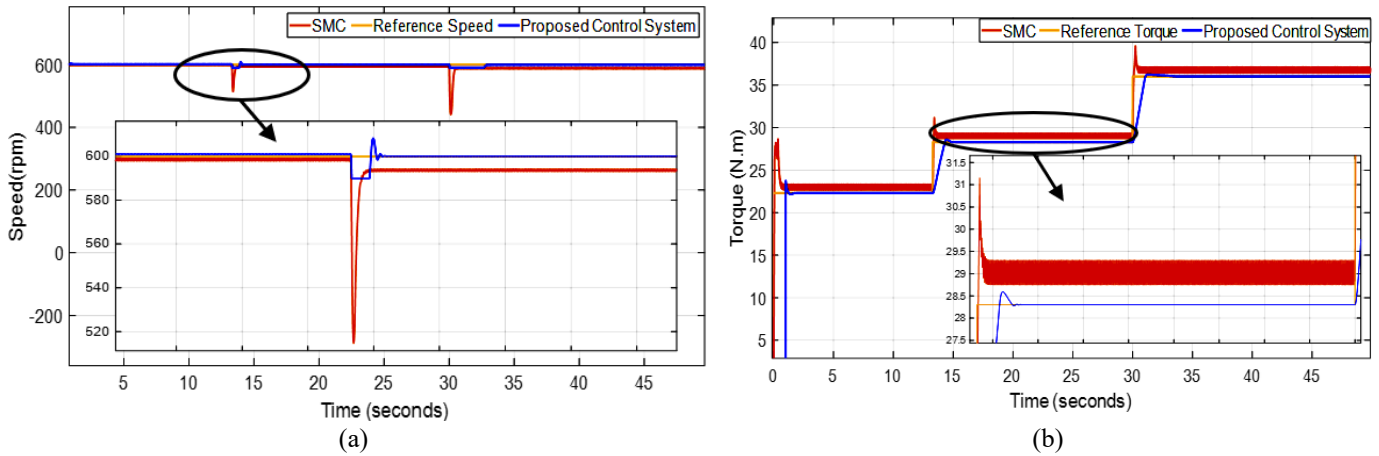


Figure 6. Experimental results: System response during second scenario (constant speed and variable torque) (a) speed response, (b) torque response

Figure 7 shows the results for the second scenario, a constant speed with variable torque, the proposed control system superior performance is evident in its armature current, field current, output DC/DC converter voltage, and output power responses. Figure 7(a) shows the armature current response. The proposed control system (blue line) draws a higher armature current as the torque demand increases. For a reference torque of 30 N.m, the proposed system's armature current is approximately 32 A, while the conventional SMC's current is about 26 A. When the torque is increased further, the proposed system's current rises to approximately 37 A, while the conventional SMC's current reaches around 30 A. The proposed control system handles the torque steps with a faster and smoother transition compared to the conventional SMC.

Figure 7(b) shows the field current. The proposed control system field current (blue line) remains at a lower and more constant level, at approximately 0.85 A, even when the torque demand changes. In contrast the conventional SMC field current (red line) remains higher at approximately reach to 1.07 A. The output DC/DC converter voltage in Figure 7(c) shows the significant difference in power stage performance. The proposed system voltage response is consistently smoother with less ripple and faster settling times during the transitions. When the torque steps up at around 15 seconds the proposed system voltage rises smoothly to approximately 140 V. It remains stable while the conventional SMC system voltage shows that more pronounced fluctuations before

settling. The stable voltage regulation is crucial for the providing a clean power supply to the motor. Figure 7(d) shows the output power response. The proposed system requires less power to achieve the same performance as the conventional SMC. The output power for both systems tracks the changes in torque demand. When the torque increases, the power output of the proposed control system rises to approximately 5100 W, while the conventional SMC rises to about 4000 W. The proposed system consistently draws more power to precisely and smoothly follow the torque changes. That is a direct consequence of the proposed system's reduced current ripple and improved efficiency which stems from the effective mitigation of chattering by the adaptive SMC and the superior voltage regulation of the advanced boost VMS converter. The reduced ripple means less energy is wasted as heat that leading to a more efficient overall system.

3.3 Third scenario results

Figure 8 represents the third scenario of variable speed and variable torque, clearly shows the proposed control system's superior performance in handling complex dynamic changes. Figure 8(a) shows the speed response. The proposed system remarkable ability to track the reference speed with high precision, even when the reference torque is also changing. At the 15-second mark, when both speed and torque change simultaneously, the proposed system quickly settles to the new

reference speed with minimal transient deviation. The conventional SMC exhibits a larger initial overshoot and more noticeable oscillations before settling. The zoom-in view highlights this difference that showing the conventional SMC with significant speed ripple, fluctuating by approximately 10

rpm (from 815 rpm to 805 rpm) while the proposed system maintains a nearly perfect and ripple-free steady state at 805 rpm. The superior tracking and stability are a testament to the robust and the adaptive nature of the proposed control algorithm.

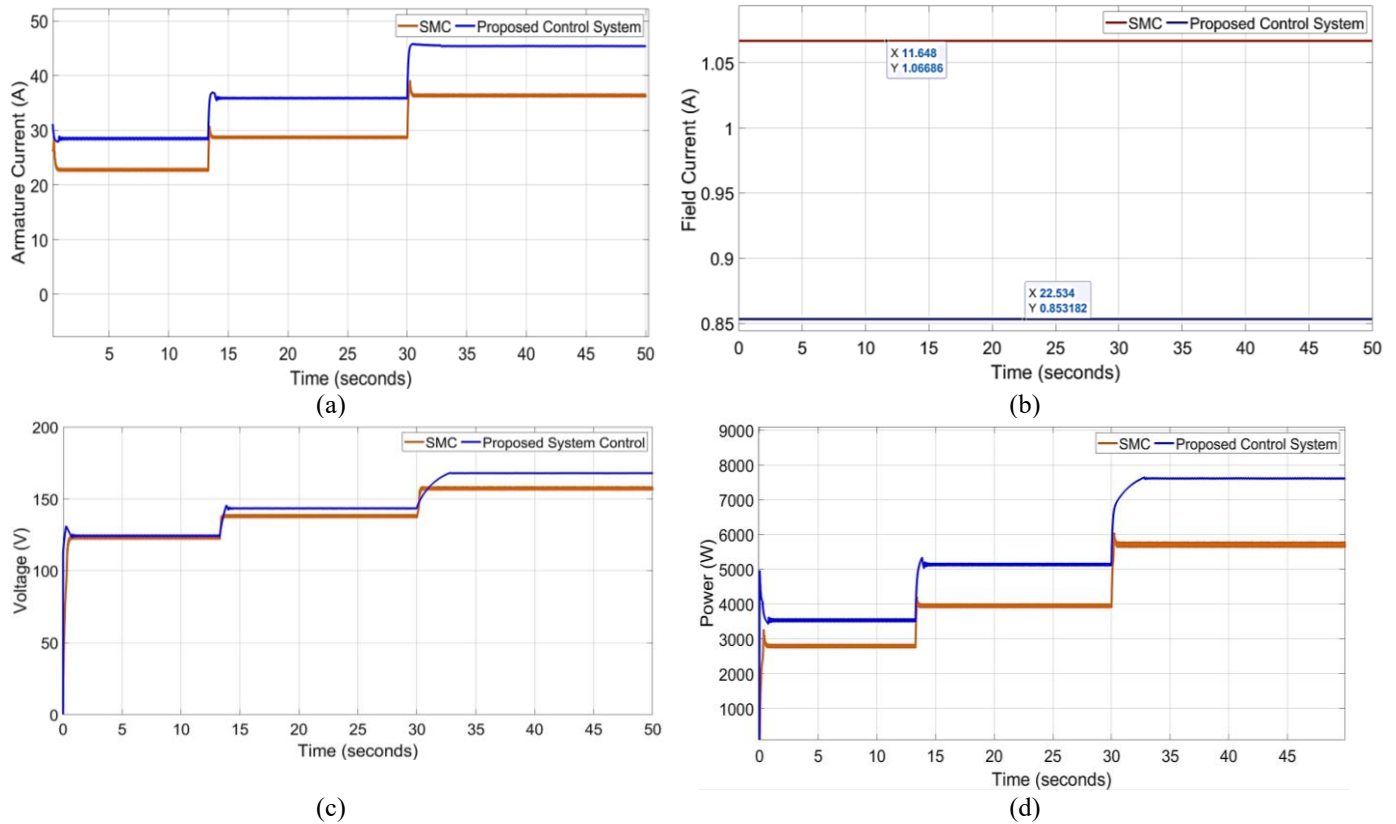


Figure 7. Experimental results: System response during second scenario (constant speed and variable torque) (a) armature current, (b) field current, (c) output DC/DC converter voltage, (d) output power

Figure 8(b) shows the torque response for the third scenario. While both controllers successfully track the reference torque steps the proposed system does so with significantly less ripple and chattering. The zoomed section reveals the conventional SMC torque output with noticeable high-frequency oscillations that fluctuating between approximately 29 N.m and 31.5 N.m when the reference torque is 30 N.m. The proposed system on the other hand maintains a much tighter torque output with minimal fluctuation. The difference is directly linked to the physical principles of the two controllers. The conventional SMC chattering a result of its switching nature that translates into high-frequency ripple in the torque output which can lead to increased stress on the motor and mechanical system. The adaptive nature of the proposed SMC minimizes this chattering by adjusting control parameters in real time that leading to a much smoother and more stable torque response. The results in not only better performance but also improved system longevity and efficiency. To quantify the torque ripple, it can use the Eq. (20):

$$\text{Torque Ripple}_{\text{SMC}} = \frac{31.5 - 29}{30} \times 100\% = 8.3\%$$

$$\begin{aligned} \text{Torque Ripple}_{\text{Proposed Control System}} &= \frac{30.2 - 29.8}{30} \times 100\% = 1.33\% \end{aligned}$$

The calculation shows that the conventional SMC has a significant torque ripple of approximately 8.33%, while the

proposed system has a substantially lower torque ripple of approximately 1.33% that confirming its superior performance in this demanding variable speed and variable torque scenario.

Figure 9 presents the results for the third scenario of variable speed and variable torque, clearly shows the proposed control system's superior performance in managing armature current, field current, output DC/DC converter voltage, and output power.

Figure 9(a) shows the armature current response. The proposed control system (blue line) consistently draws a higher armature current than the conventional SMC (red line). For instance, when the speed and torque increase the proposed system current rises to approximately 37 A, while the conventional SMC current rises to around 26 A. The proposed control system's current response is more stable and has less ripple during both steady-state operation and dynamic transitions, highlighting its superior control performance in the most challenging scenario. The physical reason for the proposed system higher armature current is likely a consequence of its control strategy which is prioritizes tracking accuracy and reduced ripple over minimal current draw. The advanced boost VMS converter ability to provide a more stable and regulated voltage output, combined with the adaptive SMC ability to minimize chattering that allows for more precise control of the motor speed and torque. The superior control while drawing a higher current that results in the significantly lower torque ripple and improved overall system performance observed in the other Figures. The

conventional SMC while drawing less current that exhibits greater oscillations and is less efficient at maintaining the desired output due to its inherent chattering. However, the proposed system (blue line) maintains a lower field current of approximately 0.85 A while the conventional SMC (red line) operates at a field current of approximately to 1.07 A. Across all three scenarios the proposed control system consistently operates at a lower field current that indicating a more efficient use of power in the field winding of the DC motor. Figure 9(c) shows the output DC/DC converter voltage. The significant

difference in the power stage performance. The proposed system voltage response is consistently smoother with less ripple and faster settling times during the transitions. When the torque and speed step up at around 15 seconds the proposed system voltage rises smoothly to approximately to 130 V and remains stable while the conventional SMC system voltage shows more pronounced fluctuations before settling. The stable voltage regulation is crucial for the providing a clean power supply to the motor.

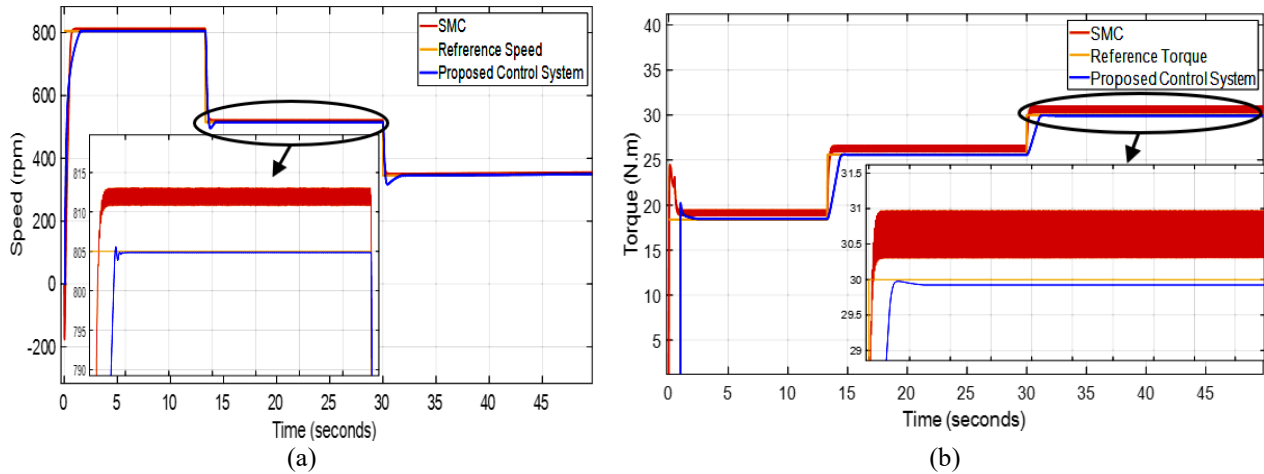


Figure 8. Experimental results: System response during third scenario (variable speed and variable torque) (a) speed response, (b) torque response

As seen in Figure 9(d) the proposed control system operates at a significantly higher power level that reaching approximately to 7600 W in contrast to the conventional SMC which reaches approximately to 5700 W. The higher power consumption by the proposed system is a necessary trade off

to achieve its superior performance in speed tracking and torque ripple reduction. The increased power draws the enables the system to maintain a stable and smooth response even under the most challenging operating conditions.

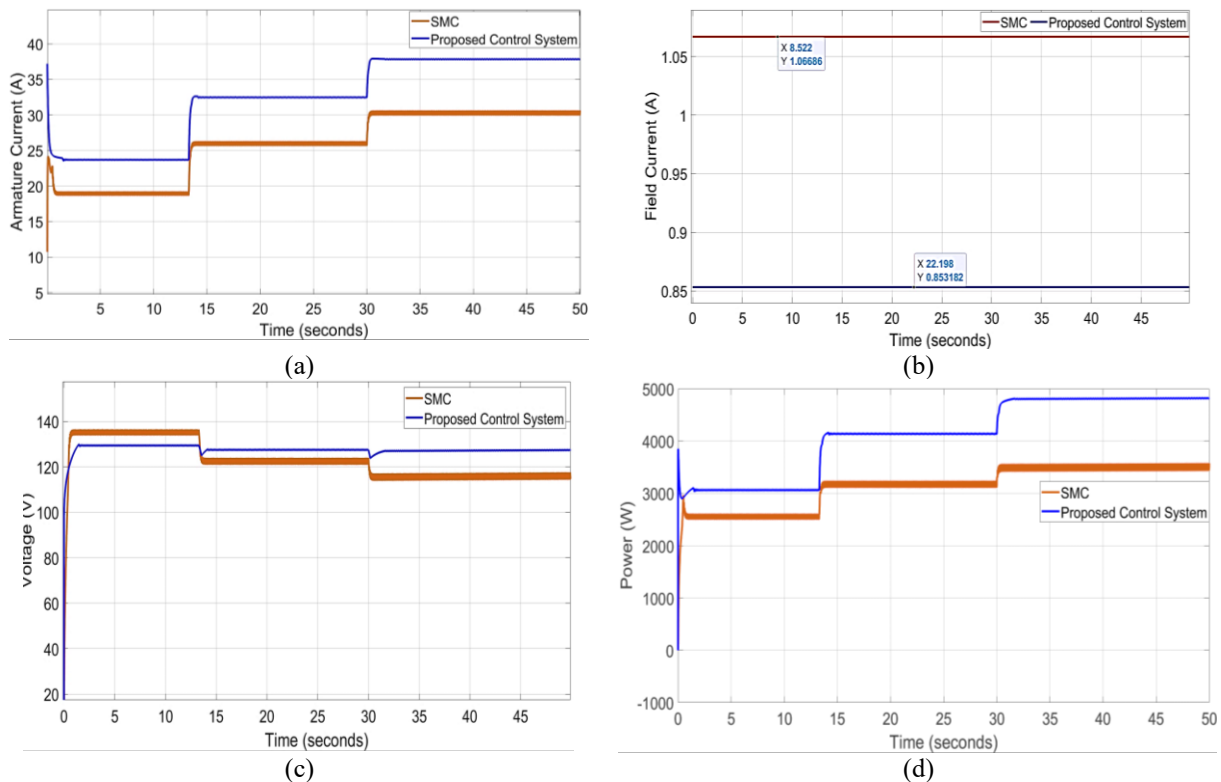


Figure 9. Experimental results: System response during third scenario (variable speed and variable torque) (a) armature current, (b) field current, (c) output DC/DC converter voltage, (d) output power

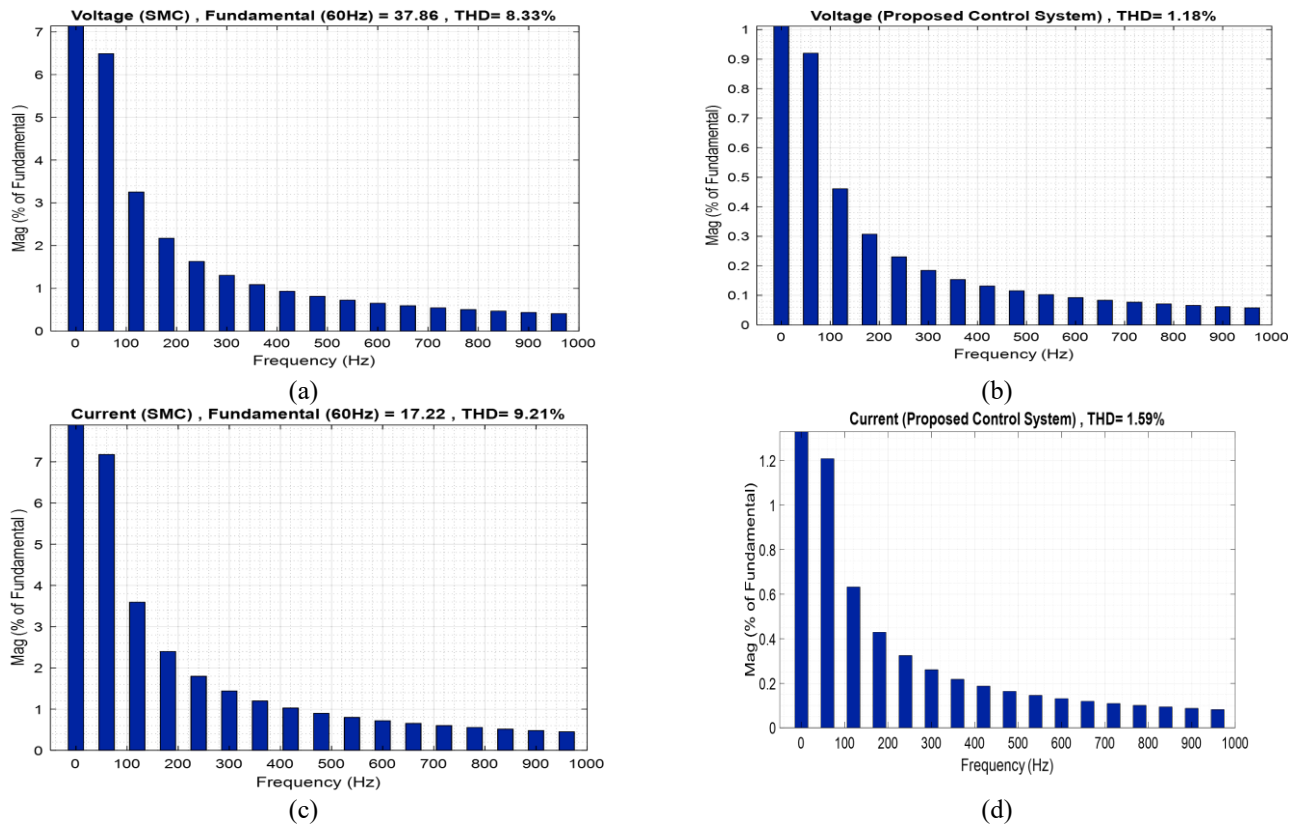


Figure 10. THD for SMC and proposed system (a) SMC voltage, (b) proposed control system voltage, (c) SMC armature current, (d) proposed control system armature current

Figure 10 shows the THD result. The proposed control system that demonstrates a stark and physically significant outperformance over the conventional SMC system. The conventional SMC voltage THD is calculate at a high 8.33% while its armature current THD is even high at 9.21%. In stark contrast the proposed control system achieves a remarkably low voltage THD of just 1.18% and an armature current THD of 1.59%. This is a dramatic reduction, with the proposed system's THD being approximately seven times lower for voltage and nearly six times lower for current.

The physical reasons for the superior performance lie in the fundamental design and operation of the integrated system. Conventional SMC while effective for robust control that inherently generates a significant amount of high-frequency noise and harmonics. That is due to its "chattering" phenomenon where the control signal rapidly switches back and forth at a high frequency to keep the system state on the sliding surface. The rapid switching introduces undesirable high-frequency components into the converter output voltage and, subsequently the motor armature current. These harmonics do not contribute to useful motor work but instead lead to increased losses in the motor windings that excessive heating, and potential for electromagnetic interference (EMI). The high THD values for the conventional SMC are a direct quantitative measure of the ripple and chattering.

The proposed control system outperformance is a direct consequence of two key factors working in synergy. First the adaptive nature of the SMC is designed to mitigate the chattering effect. By dynamically adjusting the control parameters the adaptive controller can provide a smoother control signal that reducing the high-frequency switching and, as a result the harmonic content. Secon and perhaps most importantly the advanced boost VMS converter provides a cleaner power supply. Unlike a conventional converter that

might have inherent ripple the VMS converter is optimized for precise output voltage regulation. It actively shapes the output voltage to be as close as possible to the desired DC value thereby filtering out the harmonics that would otherwise be present. The combination of an intelligent adaptive control algorithm that minimizes chattering and a high-fidelity power stage that cleans up the output signal results in a near ideal DC power supply for the motor. That is leading to the very low THD values observed which translates to a more efficient, quieter, and reliable motor drive with reduced losses and improved longevity.

The summary of the research results in a Table 3.

Table 3. Summary of research results

Parameter	Conventional SMC	Proposed Control System
Scenario 1: torque ripple	15%	5%
Scenario 2: torque ripple	10%	1.33%
Scenario 3: torque ripple	8.33%	1.33%
Voltage THD	8.33%	1.18%
Current THD	9.21%	1.59%

The calculation for the measure of the system's ability to maintain a stable speed with minimal fluctuation. It is quantified as the percentage of the average speed that is free from ripple. The formula used is:

$$Tracking\ Efficiency = \left(1 - \frac{Speed_{ripple}}{Speed_{average}}\right) \times 100\% \quad (21)$$

Speed tracking efficiency is calculated as the percentage of the reference speed that is accurately maintained, which is a measure of the system ability to minimize ripple and oscillations. The calculation is based on the speed ripple observed in the steady-state portion of the graphs from the first scenario:

$$\text{Tracking Efficiency}_{SMC} = \left(1 - \frac{30}{800}\right) \times 100\% = 96.25\%$$

$$\begin{aligned} \text{Tracking Efficiency}_{\text{Proposed Control System}} \\ = \left(1 - \frac{2}{800}\right) \times 100\% = 99.75\% \end{aligned}$$

The calculation of tracking efficiency for the third scenario is given:

$$\text{Tracking Efficiency}_{SMC} = \left(1 - \frac{10}{805}\right) \times 100\% = 98.75\%$$

$$\begin{aligned} \text{Tracking Efficiency}_{\text{Proposed Control System}} \\ = \left(1 - \frac{1}{805}\right) \times 100\% = 99.88\% \end{aligned}$$

Table 4 shows the summary of the comparative in dynamic performance between SMC and proposed control system.

Table 4. Summary of dynamic performance

Parameter	Conventional SMC	Proposed Control System
Rise time (s)	0.35	0.15
Settling time (s)	0.6	0.25
Speed tracking efficiency (Scenario 1)	96.25%	99.75%
Speed tracking efficiency (Scenario 3)	98.75%	99.88%

According to Table 5 which compares the research with earlier investigations the suggested control system responds better than other types. It primarily serves to benchmark the potential improvement offered by the proposed Adaptive SMC strategy against established techniques under their respective optimal or typical operating conditions rather than providing a direct side-by-side quantitative comparison under a single that unified test protocol.

Table 5. Comparative analysis of dynamic performance for various dc motor control systems

Previous Studies	Rise Time (s)	Settling Time (s)
Proposed control system	0.15	0.25
Conventional SMC with boost converter	0.35	0.35
SMC [10]	0.593	1.627
PID [10]	1.422	6.707
Fuzzy logic control (FLC) [10]	1.135	2.165

4. CONCLUSION

This research successfully demonstrates the significant performance advantages of a novel control system for the DC

motors that synergistically combines ASMC with an advanced boost VMS converter. The study findings that supported by comprehensive numerical analysis across three distinct operating scenarios that prove that this integrated approach effectively addresses the key limitations of conventional control methods. By dynamically adapting to system uncertainties and providing a remarkably clean power supply the proposed system drastically reduces undesirable effects such as chattering, high-frequency ripple and harmonics. That is quantitatively evidenced by the substantial reduction in THD with voltage THD dropping from 8.33% to 1.18% and current THD from 9.21% to 1.59% compared to the conventional SMC. Moreover, the system exhibits superior dynamic response that achieving faster settling times (as low as 0.25 seconds) and significantly that improving speed tracking efficiency to over 99.8%. The minimal torque ripple that reduced to as little as 1.33% in the most challenging scenarios further confirms the system robustness and precision. The results collectively validate the proposed system as a highly efficient, stable and robust solution for high performance DC motor control that validating its potential for demanding industrial and robotic applications.

4.1 Limitations and future work

A notable limitation of this study is that the validation was exclusively simulation-based that meaning the exact performance degradation due to real-world hardware constraints such as time delays, power component non-idealities and measurement noise that remains unquantified. Building upon this success the following directions are proposed for future research:

1. Transitioning the control system from simulation to the physical prototype. That involves optimizing the ASMC algorithm for execution on high-speed platforms like DSPs or FPGAs to meet the strict timing requirements imposed by the adaptive gain updates which is a significant computational challenge.
2. Investigating intelligent control methods such as fuzzy logic or neural networks to design the adaptation gain. That would allow the controller to learn from real-world operating data potentially offering a more refined and robust chattering mitigation strategy than the current fixed-power law.
3. Exploring advanced techniques to decrease the output needed power for the proposed control system without sacrificing the achieved performance metrics thereby improving overall system efficiency.
4. Designing an observer-based ASMC to estimate unmeasurable states or the external system disturbances. That would further enhance the controller robustness in practical settings where direct state sensing is infeasible.

5. Conducting a rigorous comparative study against other state of the art controllers such as Higher Order SMC or Adaptive Backstepping Control to clearly define the specific niche where the proposed ASMC with an advanced VMS converter excels.

REFERENCES

[1] Oshaba, A.S., Ali, E.S., Abd Elazim, S.M. (2017). PI controller design using ABC algorithm for MPPT of PV system supplying DC motor pump load. Neural Computing and Applications, 28(2): 353-364.

- <https://doi.org/10.1007/s00521-015-2067-9>
- [2] Abed, M.A.N., Altahir, A.A.R., Abdulhadi, A.P.D.A.A. (2024). Review of hybrid electric vehicle configurations: advances and challenges. *Kerbala Journal for Engineering Science*, 4(3). <https://kjes.uokerbala.edu.iq>.
 - [3] Rahayu, E.S., Ma'arif, A., Cakan, A. (2022). Particle swarm optimization (PSO) tuning of PID control on DC motor. *International Journal of Robotics and Control Systems*, 2(2): 435-447. <https://doi.org/10.31763/ijrcs.v2i2.476>
 - [4] Okoro, I.S., Enwerem, C.O. (2020). Robust control of a DC motor. *Heliyon*, 6(12): e05777. <https://doi.org/10.1016/j.heliyon.2020.e05777>
 - [5] Wang, T., Wang, H., Hu, H., Wang, C. (2020). LQR optimized BP neural network PI controller for speed control of brushless DC motor. *Advances in Mechanical Engineering*, 12(10): 1687814020968980. <https://doi.org/10.1177/1687814020968980>
 - [6] Tarusan, S.A.A., Jidin, A., Huzainirah, I., Rahim, M.K., Karim, K.A. (2016). DTC brushless DC motor by using constant switching frequency. In 2016 IEEE International Conference on Power and Energy (PECon), Melaka, Malaysia, pp. 205-209. <https://doi.org/10.1109/PECON.2016.7951560>
 - [7] Jiao, Y. (2012). Advanced control methods and topologies for DC-DC power conversion (Doctoral dissertation).
 - [8] Nagarajan, R., Sathishkumar, S., Balasubramani, K., Boobalan, C., Naveen, S., Sridhar, N. (2016). Chopper fed speed control of DC motor using PI controller. *IOSR Journal of Electrical and Electronics Engineering*, 11(3): 65-69. <https://doi.org/10.9790/1676-1103016569>
 - [9] Sahputro, S.D., Fadilah, F., Wicaksono, N.A., Yusivar, F. (2017). Design and implementation of adaptive PID controller for speed control of DC motor. In 2017 15th International Conference on Quality in Research (QIR): International Symposium on Electrical and Computer Engineering, Nusa Dua, Bali, Indonesia, pp. 179-183. <https://doi.org/10.1109/QIR.2017.8168478>
 - [10] Habib, H.U.R., Waqar, A., Junejo, A.K., Elmorshedy, M.F., Wang, S., Bükér, M.S., Kim, Y.S. (2021). Optimal planning and EMS design of PV based standalone rural microgrids. *IEEE Access*, 9: 32908-32930. <https://doi.org/10.1109/ACCESS.2021.3060031>
 - [11] Masoudi, H., Kiyomarsi, A., Madani, S.M., Ataei, M. (2023). Closed-loop direct power control of brushless dc motor in field weakening region. *IEEE Transactions on Transportation Electrification*, 10(2): 3482-3491. <https://doi.org/10.1109/TTE.2023.3305050>
 - [12] Abed, M.A.N., Hashim, N.M., Nasar, Y., Hanfesh, A.O., Altahir, A.A.R. (2025). Genetic algorithm-tuned PID for Sensorless PMSM speed control using a second-order sliding mode observer. *Journal of Robotics and Control*, 6(5): 2565-2580. <https://doi.org/10.18196/jrc.v6i5.27013>
 - [13] Arshad, M.H., Abido, M.A. (2021). Hierarchical control of DC motor coupled with Cuk converter combining differential flatness and sliding mode control. *Arabian Journal for Science and Engineering*, 46(10): 9413-9422. <https://doi.org/10.1007/s13369-020-05305-9>
 - [14] Devanshu, A., Singh, M., Kumar, N. (2019). An improved nonlinear flux observer based sensorless FOC IM drive with adaptive predictive current control. *IEEE Transactions on Power Electronics*, 35(1): 652-666. <https://doi.org/10.1109/TPEL.2019.2912265>
 - [15] Konstantopoulos, G.C., Alexandridis, A.T. (2015). Enhanced control design of simple DC-DC Boost converter-driven DC motors: Analysis and implementation. *Electric Power Components and Systems*, 43(17): 1946-1957. <https://doi.org/10.1080/15325008.2015.1070383>
 - [16] Ismail, A.A.A., Elnady, A. (2019). Advanced drive system for DC motor using multilevel DC/DC buck converter circuit. *IEEE Access*, 7: 54167-54178. <https://doi.org/10.1109/ACCESS.2019.2912315>
 - [17] Rigatos, G., Siano, P., Wira, P., Sayed-Mouchaweh, M. (2016). Control of DC-DC converter and DC motor dynamics using differential flatness theory. *Intelligent Industrial Systems*, 2(4): 371-380. <https://doi.org/10.1007/s40903-016-0061-x>
 - [18] Silva-Ortigoza, R., Hernández-Guzmán, V.M., Antonio-Cruz, M., Muñoz-Carrillo, D. (2014). DC/DC buck power converter as a smooth starter for a DC motor based on a hierarchical control. *IEEE Transactions on Power Electronics*, 30(2): 1076-1084. <https://doi.org/10.1109/TPEL.2014.2311821>
 - [19] Abed, M.A.N., Al Hakeem, Z.S., Yasir, M.S., Hanfesh, A.O. (2025). Boosting energy for building-integrated photovoltaic cells using novel boost converter with voltage multiplier cell and ANN-MPPT. *Journal of Robotics and Control (JRC)*, 6(5): 2212-2227. <https://doi.org/10.18196/jrc.v6i5.26854>
 - [20] Montoya-Acevedo, D., Gil-Gonzalez, W., Montoya, O.D., Restrepo, C., González-Castaño, C. (2024). Adaptive speed control for a DC motor using DC/DC converters: An inverse optimal control approach. *IEEE Access*, 12: 154503-154513. <https://doi.org/10.1109/ACCESS.2024.3482982>
 - [21] Alkhafaji, M.J.A., Mohammed, R.N., Mohammed, H.C., Abed, M.A.N. (2025). A Lightweight 1D CNN for unified real-time communication signal classification and denoising in low-SNR edge environments. *Buletin Ilmiah Sarjana Teknik Elektro*, 7(3): 496-508. <https://journal2.uad.ac.id/index.php/biste/article/view/13789>
 - [22] Hammoodi, S.J., Flayyih, K.S., Hamad, A.R. (2020). Design and implementation speed control system of DC motor based on PID control and matlab simulink. *International Journal of Power Electronics and Drive Systems*, 11(1): 127-134. <https://doi.org/10.11591/ijpeds.v11.i1.pp127-134>
 - [23] Ma'arif, A., Setiawan, N.R. (2021). Control of DC motor using integral state feedback and comparison with PID: Simulation and arduino implementation. *Journal of Robotics and Control*, 2(5): 456-461. <https://doi.org/10.18196/jrc.25122>
 - [24] Zafar, Z.U.A., Ali, N., Tunç, C. (2021). Mathematical modeling and analysis of fractional-order brushless DC motor. *Advances in Difference Equations*, 2021(1): 433. <https://doi.org/10.1186/s13662-021-03587-3>
 - [25] Fonov, D.A., Meshchikhin, I.A., Korzhov, E.G. (2019). Mathematical modeling of DC motors for the construction of prostheses. In *The International Symposium on Computer Science, Digital Economy and Intelligent Systems*, pp. 16-27. https://doi.org/10.1007/978-3-030-39216-1_2
 - [26] Hanfesh, A.J.O., Mohammed, J., Salman, I., Mohammed, H., Ali, M. (2024). Design and

- implementation of a solar tracking system using a hydraulic system. AIP Conference Proceedings, 3002(1): 050001. <https://doi.org/10.1063/5.0205799>
- [27] Hameed, K.R., Suraiji, A.L., Hanfesh, A.O. (2024). Comparative the effect of distribution transformer coil shape on electromagnetic forces and their distribution using the FEM. Open Engineering, 14(1): 20220503. <https://doi.org/10.1515/eng-2022-0503>
- [28] Semenov, A.S., Khubieva, V.M., Kharitonov, Y.S. (2018). Mathematical modeling of static and dynamic modes DC motors in software package MATLAB. In 2018 International Russian Automation Conference (RusAutoCon) Sochi, Russia, pp. 1-5. <https://doi.org/10.1109/RUSAUTOCON.2018.8501666>
- [29] Abed Alkhafaji, M.J., Kashkevich, S., Shyshatskyi, A., Sova, O., Nalapko, O., Buyalo, O., Dvorskyi, M. (2024). Development of a method for managing a group of unmanned aerial vehicles using a population algorithm. Eastern-European Journal of Enterprise Technologies, 132(9). <https://doi.org/10.15587/1729-4061.2024.318600>
- [30] Shetty, P., Subramonium, A.N., Kumar, M.S. (2015). Mathematical modeling of permanent magnet brushless dc motor for electric scooter. In 2015 Fifth International Conference on Communication Systems and Network Technologies, Gwalior, India, pp. 1222-1226. <https://doi.org/10.1109/CSNT.2015.110>
- [31] Rakhonde, S., Kulkarni, V. (2018). Sliding mode controller (SMC) governed speed control of DC motor. In 2018 3rd IEEE International Conference on Recent Trends in Electronics, Information Communication Technology (RTEICT), Bangalore, India, pp. 1657-1662. <https://doi.org/10.1109/RTEICT42901.2018.9012572>
- [32] Saputra, D.D., Ma'arif, A., Maghfiroh, H., Baballe, M.A., Tusset, A.M., Sharkawy, A.N., Majdoubi, R. (2023). Performance evaluation of sliding mode control (SMC) for dc motor speed control. Jurnal Ilmiah Teknik Elektro Komputer dan Informatika, 9(2): 502-510. <http://doi.org/10.26555/jitek.v9i2.26291>
- [33] Abed, M.A.N., Altahir, A.A.R., Hanfesh, A.O., Ahmed, A.A. (2024). Performance evaluation of PMSM and BLDC motors in different operating scenarios-based slide mode control. In 2024 4th International Conference on Electrical Machines and Drives (ICEMD), Tehran, Iran, Islamic Republic of, pp. 1-7. <https://doi.org/10.1109/ICEMD64575.2024.10963593>
- [34] Zaihidee, F.M., Mekhilef, S., Mubin, M. (2018). Fractional order SMC for speed control of PMSM. In 2018 International Electrical Engineering Congress (iEECON), Krabi, Thailand, pp. 1-4. <https://doi.org/10.1109/IEECON.2018.8712281>
- [35] Abed, M.A.N., Shanan, D.S., Alhussein, Z.H.H. (2025). A robust speed and torque control of DC Motor with Cuk converter using PI and SMC. Journal of Robotics and Control, 6(3): 1216-1226. <https://doi.org/10.18196/jrc.v6i3.25756>
- [36] Abed Alkhafaji, M.J., Kuchuk, N., Stanovska, I., Artabaiev, Y., Nechyporuk, O., Voznytsia, A., Rybitskyi, O. (2024). THE Development of a Method for Increasing the Reliability of the Assessment of the State of the Object. Eastern-European Journal of Enterprise Technologies, 131(3): <https://doi.org/10.15587/1729-4061.2024.313934>
- [37] Jadallah, A.A., Hanfesh, A.O., Jebur, T.H. (2018). Design, fabrication, testing and simulation of a modern glass to glass photovoltaic module in Iraq. Journal of Engineering Science and Technology, 13(9): 2750-2764.
- [38] Majdi, H.S., Shijer, S.S., Hanfesh, A.O., Habeeb, L.J., Sabry, A.H. (2021). Analysis of Fault diagnosis of DC motors by Power Consumption Pattern Recognition. European Journal of Enterprise Technologies, 5(5): 113. <https://doi.org/10.15587/1729-4061.2021.240262>
- [39] Kollabathula, P., Padma, K. (2017). Speed control of DC motor using adaptive PID with SMC scheme. International Research Journal of Engineering and Technology, 4(09): 163-170.
- [40] Kumar, T.D., Mija, S.J. (2015). Dynamic SMC control scheme with adaptively tuned PID controller for speed control of DC motor. In 2015 IEEE International Conference on Industrial Technology (ICIT), Seville, Spain, pp. 187-191. <https://doi.org/10.1109/ICIT.2015.7125097>
- [41] Qi, W., Zong, G., Karim, H.R. (2018). Observer-based adaptive SMC for nonlinear uncertain singular semi-Markov jump systems with applications to DC motor. IEEE Transactions on Circuits and Systems I: Regular Papers, 65(9): 2951-2960. <https://doi.org/10.1109/TCSI.2018.2797257>
- [42] Taleb, M., Plestan, F., Bououlid, B. (2014). Higher order sliding mode control based on adaptive first order sliding mode controller. IFAC Proceedings Volumes, 47(3): 1380-1385. <https://doi.org/10.3182/20140824-6-ZA-1003.02487>
- [43] Fan, X., Sun, H., Yuan, Z., Li, Z., Shi, R., Ghadimi, N. (2020). High voltage gain DC/DC converter using coupled inductor and VM techniques. IEEE Access, 8: 131975-131987. <https://doi.org/10.1109/ACCESS.2020.3002902>
- [44] Mohseni, P., Mohammadsalehian, S., Islam, M.R., Muttaqi, K.M., Sutanto, D., Alavi, P. (2021). Ultrahigh voltage gain DC-DC boost converter with ZVS switching realization and coupled inductor extendable voltage multiplier cell techniques. IEEE Transactions on Industrial Electronics, 69(1): 323-335. <https://doi.org/10.1109/TIE.2021.3050385>
- [45] Hadi, N.J., Al-Tahir, A.A.R. (2010). Study of thermal solar energy storage using stationary batteries and melting salts technique. Journal of Babylon University/Pure and Applied Sciences, 18(1): 365-379.
- [46] Zhu, B., Hu, S., Liu, G., Huang, Y., She, X. (2020). Low-voltage stress buck-boost converter with a high-voltage conversion gain. IEEE Access, 8: 95188-95196. <https://doi.org/10.1109/ACCESS.2020.2995889>
- [47] Andrade, A.M.S.S., Mattos, E., Schuch, L., Hey, H.L., da Silva Martins, M.L. (2017). Synthesis and comparative analysis of very high step-up DC-DC converters adopting coupled-inductor and voltage multiplier cells. IEEE Transactions on Power Electronics, 33(7): 5880-5897. <https://doi.org/10.1109/TPEL.2017.2742900>